Theor Appl Climatol
DOI 10.1007/s00704-014-1201-4

ORIGINAL PAPER

Designing laboratory wind simulations using artificial neural networks

Josip Križan · Goran Gašparac · Hrvoje Kozmar · Oleg Antonić · Branko Grisogono

Received: 11 February 2014 / Accepted: 5 June 2014

Abstract While experiments in boundary layer wind tunnels remain to be a major research tool in wind engineering and environmental aerodynamics, designing the modeling hardware required for a proper atmospheric boundary layer (ABL) simulation can be costly and time consuming. Hence, possibilities are sought to speed-up this process and make it more time-efficient. In this study, two artificial neural networks (ANNs) are developed to determine an optimal design of the Counihan hardware, i.e., castellated barrier wall, vortex generators, and surface roughness, in order to simulate the ABL flow developing above urban, suburban, and rural terrains, as previous ANN models were created for one terrain type only. A standard procedure is used in developing those two ANNs in order to further enhance best-practice possibilities rather than to improve existing ANN designing methodology. In total, experimental results obtained using 23 different hardware setups are used when creating ANNs. In those tests, basic barrier height, barrier castellation height, spacing density, and height of surface roughness elements are the parameters that were varied to create satisfactory ABL simulations. The first ANN was used for the estimation of mean wind velocity, turbulent Reynolds stress, turbulence intensity, and length scales, while the second one was used for the estimation of the power spectral density of velocity fluctuations. This extensive set of studied flow and turbulence parameters is unmatched in comparison to the previous relevant studies, as it includes here turbulence intensity and power spectral density of velocity fluctuations in all three directions, as well as the Reynolds stress profiles and turbulence length scales. Modeling results agree well with experiments for all terrain types, particularly in the lower ABL within the height range of the most engineering structures, while exhibiting sensitivity to abrupt changes and data scattering in profiles of wind-tunnel results. The proposed approach allows for quicker and more effective achieving targeted flow and turbulence features of the ABL wind-tunnel simulations as compared to the common trial and error procedures. This methodology is expected to enable wind-tunnel modelers a quick and time-efficient designing of ABL simulations in studies dealing with air pollutant dispersion, wind loading of structures, wind energy, and urban micrometeorology, where atmospheric flow and turbulence play a key role.

1 Introduction

Wind-tunnel experiments represent a major tool in studying wind loading of structures, air pollutant dispersion, efficiency of wind energy farms, and urban micrometeorology. As a prerequisite to those studies, it is required to precisely simulate the atmospheric boundary layer (ABL) flow that is expected to correspond to a small-scale of atmospheric conditions. The Counihan (1969) and Irwin (1981) methods that use a barrier, spires, and surface roughness are perhaps the most common approaches to simulate the ABL flow experimentally. As the wind-tunnel experimental time is costly, and tuning the experimental hardware to obtain a specific ABL is time consuming, new approaches are sought that enable to quickly achieve the targeted ABL simulation. Hence, artificial neural networks

J. Križan · G. Gašparac · O. Antonić
GEKOM Ltd. Geophysical and Ecological Modeling, Trg senjskih uskoka 1-2, 10000 Zagreb, Croatia

H. Kozmar (✉)
Faculty of Mechanical Engineering and Naval Architecture, University of Zagreb, Ivana Lučića 5, 10000 Zagreb, Croatia
e-mail: hkozmar@fsb.hr

O. Antonić
Department of Biology, Josip Juraj Strossmayer University of Osijek, Cara Hadrijana 8/A, 31000 Osijek, Croatia

B. Grisogono
Department of Geophysics, Faculty of Science, University of Zagreb, Horvatovac 95, 10000 Zagreb, Croatia

Published online: 28 June 2014

(ANNs) are considered to become a valuable tool in rapid achieving of targeted flow and turbulence features of the ABL wind-tunnel simulation that is a necessary prerequisite for successful studies dealing with air pollutant dispersion, wind loading of structures, wind energy, and urban micrometeorology and microclimatology.

Previous studies have already indicated capabilities of ANN to solve wind engineering problems. Khanduri et al. (1997) developed a neural network approach for the assessment of wind-induced interference effects on design loads for buildings. English and Fricke (1999), Huang and Gu (2005), and Xie and Gu (2005) applied neural network methodology to account for shielding and interference between buildings. Bitsuamlak et al. (2006, 2007) developed an approach to investigate speed-up ratios for topographic features such as single and multiple hills, escarpments, and valleys. Kwatra et al. (2002) and Chen et al. (2003) use an ANN approach for the estimation of pressure coefficients on the gable roofs of buildings, Fu et al. (2006, 2007) to estimate wind loads on large roofs, Yasushi and Tsuruishi (2008) for the design of roof cladding of spherical domes, and Brunskill and Lubitz (2012) for wind turbine siting near obstacles. Esau (2010) suggests that ANN is a robust tool for estimation of the pollutant scalar concentration in the urban sublayer, Vujić et al. (2010) apply it for forecasting concentration of suspended particles due to traffic air pollution in urban areas, and Sousa et al. (2007) determine ozone concentrations also by using ANN. Preceding the current study, Abdi et al. (2009) model the effect of surface roughness and spire dimensions on the mean velocity and turbulence intensity profiles in experimental models of the ABL flow, while Varshney and Poddar (2012) estimate flow characteristics in urban ABL wind-tunnel simulations; they all deploy ANN.

The scope of this study is to create two ANNs that estimate a design of experimental hardware for wind-tunnel simulations of the ABL flow. One network is designed to estimate integral flow and turbulence parameters, while the other is developed to simulate the power spectral density of velocity fluctuations. The proposed approach is dedicated to work well for different terrain types, taking into account the mean wind velocity, turbulent Reynolds stress, turbulence intensity and length scales, power spectra of velocity fluctuations, i.e., the parameters all considered to significantly determine wind loading of structures, air pollutant dispersion, wind farming, and urban micrometeorology as such (e.g., Baklanov et al. 2011). Hence, this extensive set of flow and turbulence parameters addressed is unmatched in comparison to previous relevant studies, as it includes turbulence intensity and power spectral density of velocity fluctuations in all three directions, as well as the Reynolds stress profiles and turbulence length scales. In addition, ANNs are designed to make good estimates for different terrain types, while previous studies were performed for one terrain type only.

2 Experimental simulation of the atmospheric boundary layer

Experimental ABL simulations used for validation of developed ANNs were carried out in a 1.80-m high, 2.70-m wide, and 21-m long test section of the Göttingen-type low-speed boundary layer wind tunnel at the Technische Universität München (e.g., Kozmar 2011a, b, c). In this wind tunnel, the blower is driven by a 210 kW electric motor, which allows generating velocities from 1 to 30 m/s. At the inlet to the test section, the flow uniformity is achieved by means of a honeycomb, screens, and a nozzle. Preliminary tests reported turbulence intensities at the inlet cross-section less than 0.5 %, and measured mean velocities differed less than 1 %. The adjustable ceiling enables longitudinal pressure control along the wind-tunnel test section. Structural models are usually placed at a turntable, whose center is positioned 11.3 m downwind from the nozzle; measurements reported in this study were recorded at this position in 18 measuring points placed along a vertical line down the center of the turntable distributed between the surface and 1-m height.

The simulation technique, originally introduced by Counihan (1969), was based on the use of five 1-m high quarter-elliptic, constant-wedge-angle spires and a castellated barrier wall, followed by a fetch of surface roughness elements (LEGO cubes arranged in a staggered pattern on LEGO plates). In general, the uniform flow coming out of the nozzle streams over the castellated barrier wall, which provides an initial momentum defect of the flow. The main effect of the barrier is to introduce large eddies and mean shear in the wake of the barrier. Vortices with vertical axes of rotation develop around vortex generators. Surface roughness elements provide the sustained formation of boundary layer (BL) structures downstream from the vortex generators. A design of the castellated barrier wall and surface roughness elements was modified during the measurement program to allow for training and testing of the ANNs developed to estimate an optimal experimental hardware for the ABL wind-tunnel simulations using various terrain types. For the two highest measuring points (z=0.84 and 1 m, where z is height above surface), differences in recorded mean velocities were less than 2 %. Based on Schlichting and Gersten's (1997) definition that the BL thickness is a height where the average longitudinal wind velocity reaches 99 % of the free-stream velocity, it is accepted that the BL thickness in the wind tunnel is approximately equal to 1 m. These results correspond well with Balendra et al. (2002), who indicated that the thickness of ABL simulations generated using the Counihan method matches with the vortex generators' height. A blockage caused by surface roughness elements was less than 1 % in all experiments, which is well below the critical value of 5 % (Hucho 2002; Holmes 2007). An arrangement of the simulation hardware, as employed in this study, is displayed in Fig. 1.

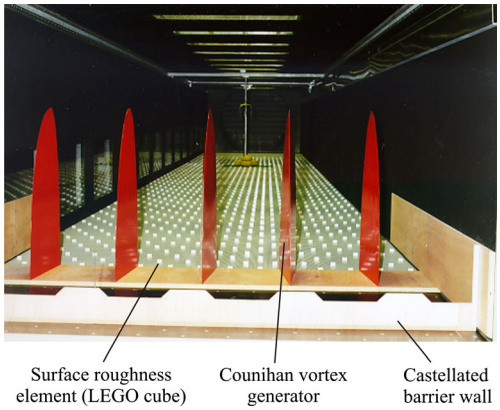

Fig. 1 Castellated barrier wall, Counihan vortex generators, and surface roughness elements in the wind-tunnel test section

Instantaneous velocities in the longitudinal x-, lateral y-, and vertical z-directions were measured using a triple hot-wire probe DANTEC 55P91. Velocity signals were sampled at 1.25 kHz using a 12-bit digitizer Data Translation DT2821 and recordings were made of 187,500 data samples at each measuring point (total record length T=150 s). Calibrations of the hot-wire probe were obtained in a calibration tunnel by exposing the probe to uniform flows with 20 different velocities and 252 different yaw angles. Tests were performed following standard wind-tunnel modeling procedures (Plate 1982; Sockel 1984) assuming a neutral stratification of the ABL flow. Roughness Reynolds number, Re_R,

$$Re_R = \frac{u_\tau \cdot z_0}{\nu}, \tag{1}$$

was larger than 5 in all tests, which is in accordance with Plate's (1982) suggestion for wind-tunnel modeling of wind effects in engineering; moreover, u_τ is friction velocity, z_0 is aerodynamic surface length, and ν is air kinematic viscosity. The BL parameters investigated in this study are given next.

The mean velocity component $\overline{u}$ in the x-direction is

$$\overline{u} = \frac{1}{T}\int_0^T u(t)dt. \tag{2}$$

Turbulence intensity in the x-, y-, and z-directions:

$$I_u(z) = \frac{\sqrt{\overline{u'^2(z)}}}{\overline{u}_z}, I_v(z) = \frac{\sqrt{\overline{v'^2(z)}}}{\overline{u}_z}, I_w(z) = \frac{\sqrt{\overline{w'^2(z)}}}{\overline{u}_z} \tag{3}$$

respectively, where

$$u(t) = \overline{u} + u'(t), v(t) = \overline{v} + v'(t), \quad \text{and } w(t) = \overline{w} + w'(t). \tag{4}$$

Note that in Eqs. (2), (3), and (4), u,v,w are instantaneous velocity components (i.e., speeds) in the x-, y-, and z-directions, $\overline{u}, \overline{v}, \overline{w}$ are mean velocity components in the x-, y-, and z-directions, and u',v',w' are the corresponding speed fluctuations in the x-, y-, and z-directions, respectively. Furthermore, $\overline{u}_z$ is the mean velocity component in the x-direction at the height of z; t is time.

Integral length scales of turbulence $L_{u,x}$, $L_{v,x}$, and $L_{w,x}$ were calculated by multiplying time scales, i.e., integrated autocorrelation coefficients, with respective $\overline{u}_z$ wind velocity and assuming the Taylor's hypothesis of frozen turbulence,

$$L_{u,x}(z) = \overline{u}_z \int_0^\infty R_{u,x}(z,\Delta t)d\Delta t, L_{v,x}(z) = \overline{u}_z \int_0^\infty R_{v,x}(z,\Delta t)d\Delta t,$$
$$L_{w,x}(z) = \overline{u}_z \int_0^\infty R_{w,x}(z,\Delta t)d\Delta t. \tag{5}$$

$R_{u,x}$, $R_{v,x}$, and $R_{w,x}$ are autocorrelation coefficients calculated as outlined in Dyrbye and Hansen (1997), and Δt is time step. Turbulence Reynolds stress was observed in the longitudinal-vertical correlation $-\overline{u'w'}$, as other correlations were observed to be close to zero. Power spectral density of velocity fluctuations $S_u(f)$, $S_v(f)$, and $S_w(f)$ was studied as well, as it is considered to be one of the key factors influencing wind loading of structures, air pollutant dispersion, efficiency of wind-energy farms, etc. In addition, a similarity of the generated BLs with full-scale conditions up to 300 to 400-m height was justified in previous studies (Kozmar 2008, 2010, 2011a, 2011b, 2011c, 2012a, 2012b), in accordance with simulation length-scale factors determined using the Cook (1978) method based on the respective turbulence length scales $L_{u,x}$ and aerodynamic surface roughness length z_0. In particular, as the presentation and discussion of results will be carried out in wind-tunnel measures, the BL thickness in the wind tunnel equals to 1 m represents 300 to 400 m in full-scale depending on a particular ABL simulation.

3 Description of applied artificial neural networks

In general, ANN represents a numerical method that simulates biological brain used for learning and recognizing patterns in data sets, as they estimate desired output data based on the provided input data. They can be used in many cases for regression and classification tasks. In this study, the estimation model was developed using the most common used type of neural networks, i.e., feed-forward multilayer perceptron (MLP) ANN, as it is in most cases an appropriate tool for regression problems, e.g., Antonić et al. (2001). ANN commonly consists of two or more layers of neurons. The output of every neuron is connected with all neurons in the next layer. Every connection has its weight and every neuron

has a bias and activation function. Weights and biases are unknown parameters that need to be obtained from training data. Prior to training, weights are initialized as proposed by Bottou (1998). In particular, for every neuron, weights are selected randomly from interval $\left[-\frac{2.38}{\sqrt{n}}, \frac{2.38}{\sqrt{n}}\right]$, where n is the number of incoming connections to the node. The output of jth neuron is calculated as $z_j=g(\sum_i a_i w_{ij}+b_j)$, where a_i is the output of ith neuron in previous layer, w_{ij} is the weight of connection from that neuron to jth neuron in the current layer, b_j is the bias of jth neuron in the current layer, and g is an activation function of jth neuron. One of the most common activation function used is a logistic sigmoid activation function given as $g(x)=1/(1+e^{-x})$, where x is an input variable. Data for each input and output parameter is linearly normalized into the range between 0.15 and 0.85 before they are presented to the ANN. Complexity of ANN depends on the number of weights and biases which depends on the number and size of hidden layers. Finding these parameters from training data is referenced as training of ANN. In this study, the *ffnet* module for the Python programming language, as given in Wojciechowski (2011), is used when creating ANN. It is a quick and easy-to-use feed-forward ANN training solution package for Python that uses a feed-forward architecture and a sigmoid activation function.

In this study, the *rprop* algorithm is used, as originally designed by Riedmiller and Braun (1993), due to its speed and simplicity. This is a widely used algorithm, especially for multilayer feed-forward networks, designed to overcome inherent disadvantages of earlier gradient-descent algorithm. If a number of parameters is too small, then ANN usually has a poor fit to training data. If a number of parameters is too large, ANN usually has a good fit to training data, but it fails to generalize to new data due to overfitting. One way to overcome this problem is a method of early stopping suggested by Bishop (1995), where the training is stopped when the error measured with respect to independent data set not used for training starts to increase. That data set is generally called a validation data set. To get an optimal ANN architecture (number of hidden layers and neurons), many instances of ANN of specific architecture using early stopping method were trained. Hence, there is a risk that the network with the best performance on validation data set might not be the one with the best performance on a new test data. Therefore, data sets used only once on every trained network were tested and a network with the best performance is chosen as the optimal one.

The performance of trained ANN is measured only on test dataset for every output parameter by using *RMSE*, *MAE*, and R^2 statistics defined as follows:

$$RMSE = \sqrt{\frac{1}{n}\sum_{i=1}^{n}(p_i - o_i)^2}, \tag{6}$$

$$MAE = \frac{1}{n}\sum_{i=1}^{n}|p_i - o_i|, \tag{7}$$

$$R^2 = 1 - \frac{\sum_{i=1}^{n}\left(p_i - \overline{p}\right)}{\sum_{i=1}^{n}\left(o_i - \overline{o}\right)}. \tag{8}$$

Here, p_i is the ith estimated value, o_i is the ith observed value, $\overline{p}$ is the average of all estimated values, and $\overline{o}$ is the average of all observed values. In Eqs. (6) through (8), *MAE* is an average of the absolute values for differences between the estimated and experimental values, while *RMSE* is a square root of the average of squared differences between estimated and experimental values. *MAE* and *RMSE* are commonly used together to diagnose the variation in the errors in an estimation set,

Table 1 Hardware arrangements in ABL wind-tunnel simulations

Test	BBH, mm	BCH, mm	SRESD, %	SREH, mm	Terrain type
2	227	42	2.8	30	S
3	107	42	2.8	30	U
4	147	42	1.4	30	U
5	147	42	1.4	40	U
6	107	42	1.4	40	S
7	227	42	1.4	40	S
8	147	42	1.4	20	S
9	107	42	1.4	20	S
10	137	42	1.4	20	S
11	127	42	1.4	20	S
12	117	42	1.4	20	S
13	107	0	1.4	20	S
14	187	0	1.4	20	S
15	107	20	1.4	20	S
16	107	60	1.4	20	S
17	107	80	1.4	20	S
18	127	42	3.5	50	U
19	127	42	0.4	30	R
20	127	42	0.6	20	R
21	107	42	0.6	20	R
22	127	42	0.4	20	R
23	127	42	3.5	30	U
24	127	42	0.2	30	R

*Numeration of tests starts with 2, as the test number 1 was a preliminary one

BBH is basic barrier height, BCH is barrier castellation height, SRESD is surface roughness elements' spacing density, SREH is surface roughness elements' height, S is suburban, U is urban, and R is rural terrain type; spectral data is available in configurations 18 to 23 only

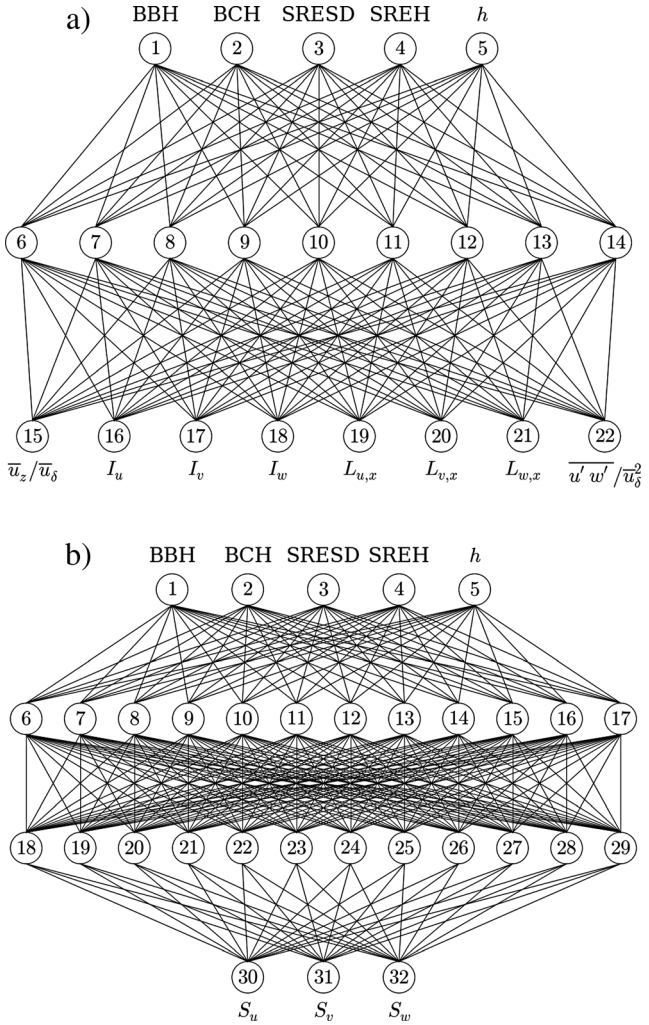

Fig. 2 Schematic view of the used artificial neural networks: **a** ANN for estimation of mean wind velocity, turbulent Reynolds stress, turbulence intensity, and length scales; **b** ANN for estimation of power spectral density of velocity fluctuations

where *RMSE* is always larger or equal to *MAE*. In particular, the larger the difference between those two parameters, the larger the variance in the individual errors in the sample. In case *RMSE* is observed to be equal to *MAE*, then all the errors are of the same magnitude. R^2 is a coefficient of determination that provides a measure how well future outcomes are likely to be estimated by the model. R^2 equals 1 indicates a perfect estimation with no error, while values close to zero indicate poor estimation.

Table 3 Performance of the second ANN

	$S_u \cdot f/\sigma_u^2$	$S_v \cdot f/\sigma_v^2$	$S_w \cdot f/\sigma_w^2$
RMSE	0.009829	0.01446	0.01565
MAE	0.006005	0.009603	0.01124
R^2	0.97	0.97	0.94

4 Results and discussion

In this study, the ability of two ANNs to estimate mean wind velocities, Reynolds stress, turbulence intensity and length scales, and power spectral density of velocity fluctuations was investigated. Both ANNs were treated for various types of terrain in order to prove a universality of the proposed approach. Experimental configurations with various combinations of the basic barrier height, barrier castellation height, and surface roughness spacing density and height are outlined in Table 1.

Design of vortex generators was the same in all tests. Length measures in all diagrams are presented at the wind-tunnel scale. It needs to be mentioned that the second ANN for power spectra estimation was not applied on suburban type of terrain due to insufficient experimental data for that terrain type. Measurements were obtained for 23 different hardware arrangements of the ABL wind-tunnel simulations (configurations), where the basic barrier height (BBH), barrier castellation height (BCH), surface roughness elements' spacing density (SRESD), and surface roughness elements' height (SREH) were varied. In each configuration, the estimated key parameters are measured in 18 different heights, i.e., at 50, 60, 71, 85, 101, 121, 144, 172, 205, 244, 291, 347, 414, 494, 589, 703, 838, and 1,000 mm. Due to technical problems with respect to velocity measurements close to surface, where the hot-wire anemometer experiences difficulties with taking measurements due to an intense recirculating flow, a few measurements were not completely reliable, so the final dataset consists a total of 412 data samples. The first ANN estimates $\overline{u}/\overline{u}_\delta$, I_u, I_v, I_w, $L_{u,x}$, $L_{v,x}$, $L_{w,x}$, $\overline{u'w'}/\overline{u}_\delta^2$, where $\overline{u}_\delta$ is the mean free-stream velocity recorded at the upper boundary of the respective simulated ABL. The input parameters are BBH, BCH, SRESD, SREH, and the height of measurement points from the surface (h). Configurations 3, 7, and 22 were used as test dataset and the rest of the data is randomly split in training and validation dataset in ratio 80:20, which led to 275

Table 2 Performance of the first ANN

	$\overline{u}/\overline{u}_\delta$	I_u	I_v	I_w	$L_{u,x}$	$L_{v,x}$	$L_{w,x}$	$\overline{u'w'}/\overline{u}_\delta^2$
RMSE	0.02684	0.005442	0.008917	0.006209	0.0511	0.01187	0.01063	0.0004451
MAE	0.01989	0.004434	0.0075	0.005142	0.0406	0.00936	0.00863	0.0003258
R^2	0.97	0.99	0.98	0.98	0.74	0.96	0.94	0.91

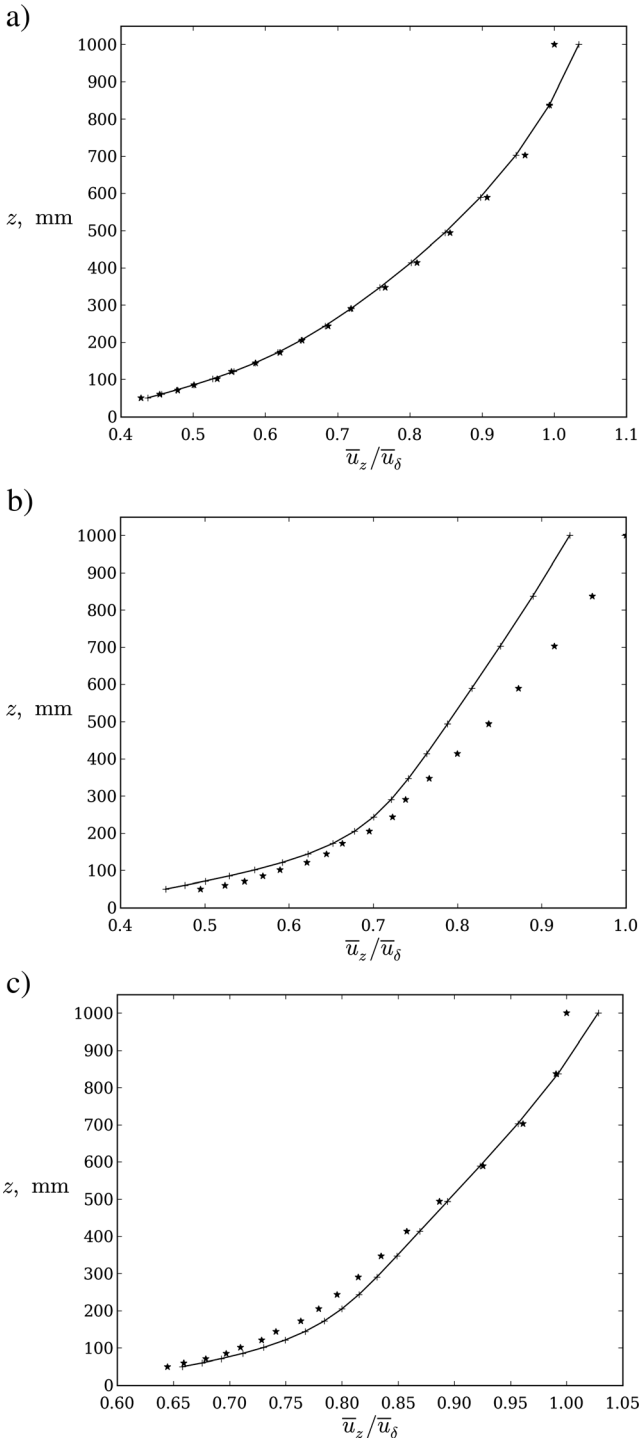

Fig. 3 Comparison of measured mean velocity profiles with values estimated by an artificial neural network for **a** urban, **b** suburban, and **c** rural terrain type; *black stars* are experimental results, and *plus signs* on a solid curve are estimated results

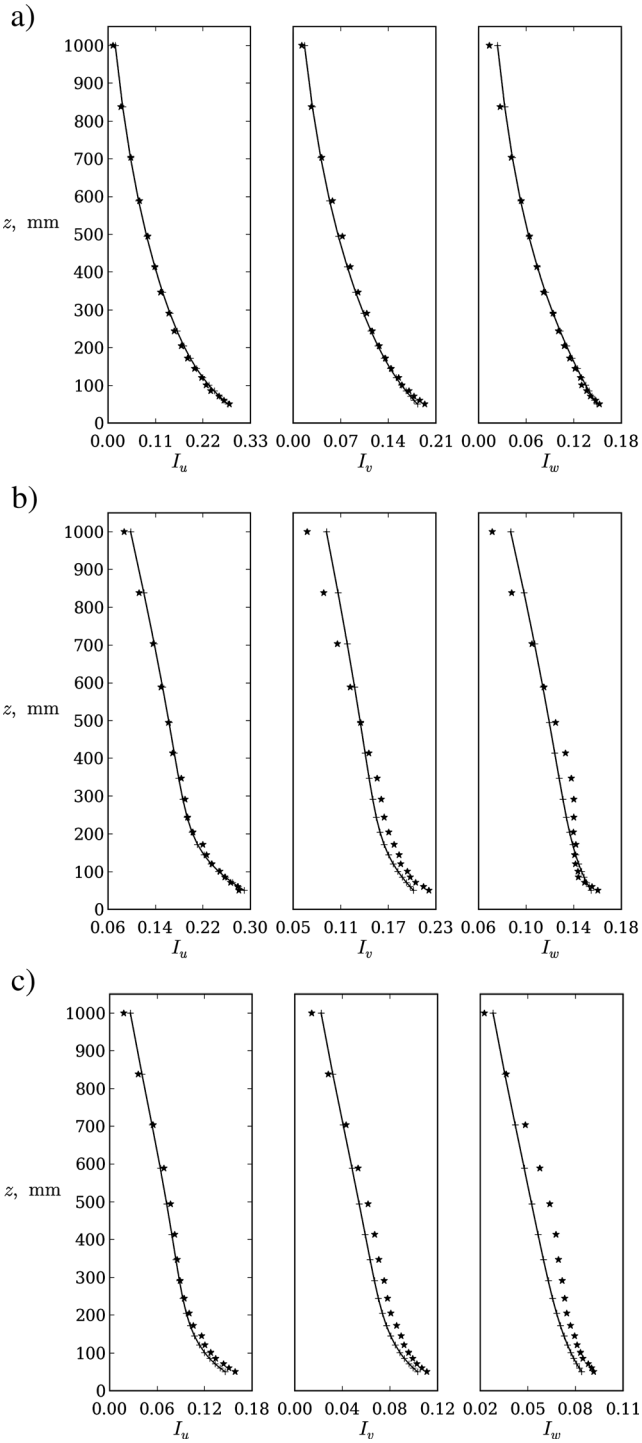

Fig. 4 Comparison of measured turbulence intensity profiles with values estimated by an artificial neural network for **a** urban, **b** suburban, and **c** rural terrain type; *black stars* are experimental results, and *plus signs* on a solid curve are estimated results

samples used for training, 83 samples used for validation, and 54 samples used as test dataset. After the procedure described in Section 3, the chosen ANN has one hidden layer with nine neurons. Schematic view of this network is displayed in Fig. 2a, and its performance is displayed in Table 2. In Table 2, $\overline{u}/\overline{u}_\delta$, I_u, I_v, I_w, $\overline{u'w'}/\overline{u}_\delta^2$, and R^2 are nondimensionalized, $L_{u,x}$, $L_{v,x}$, and $L_{w,x}$ are reported in meters, while *RMSE* and *MAE* are reported in physical units of the observed parameters, i.e., either nondimensionalized or in meters.

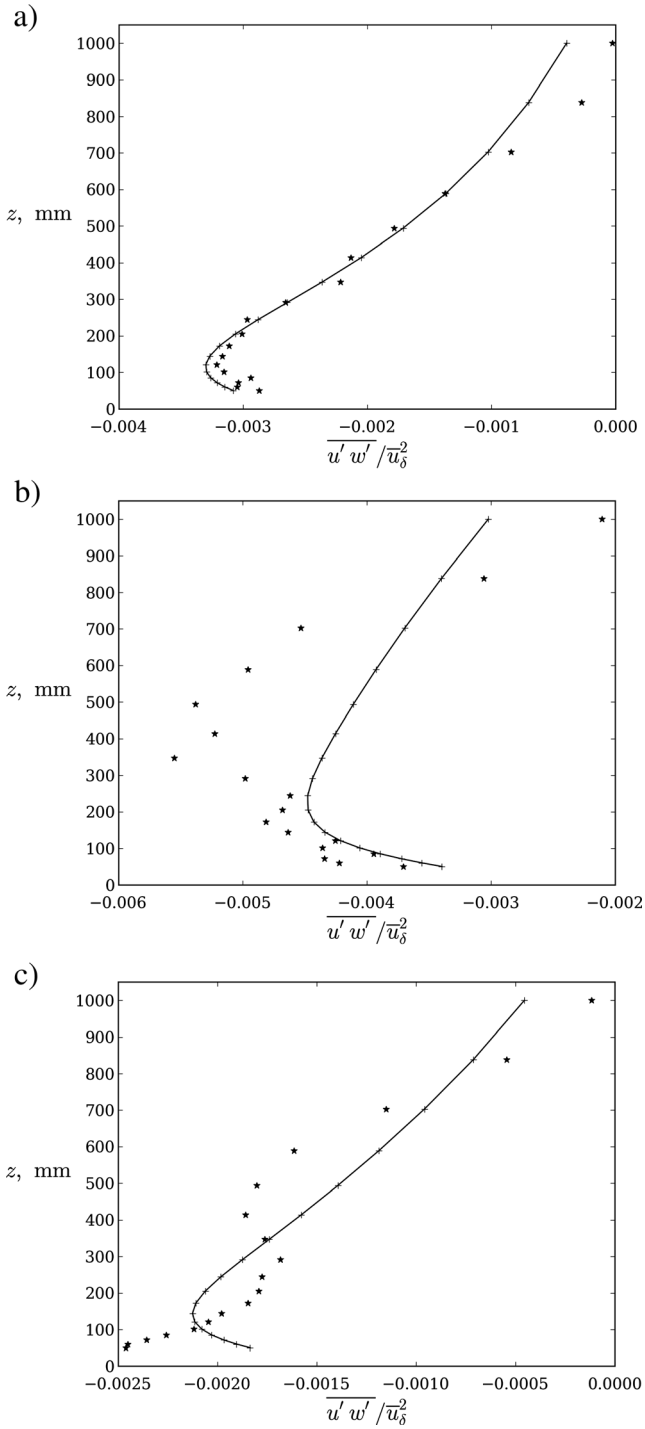

Fig. 5 Comparison of measured Reynolds stress profiles with values estimated by an artificial neural network for **a** urban, **b** suburban, and **c** rural terrain type; *black stars* are experimental results, *plus signs* on a solid curve are estimated results

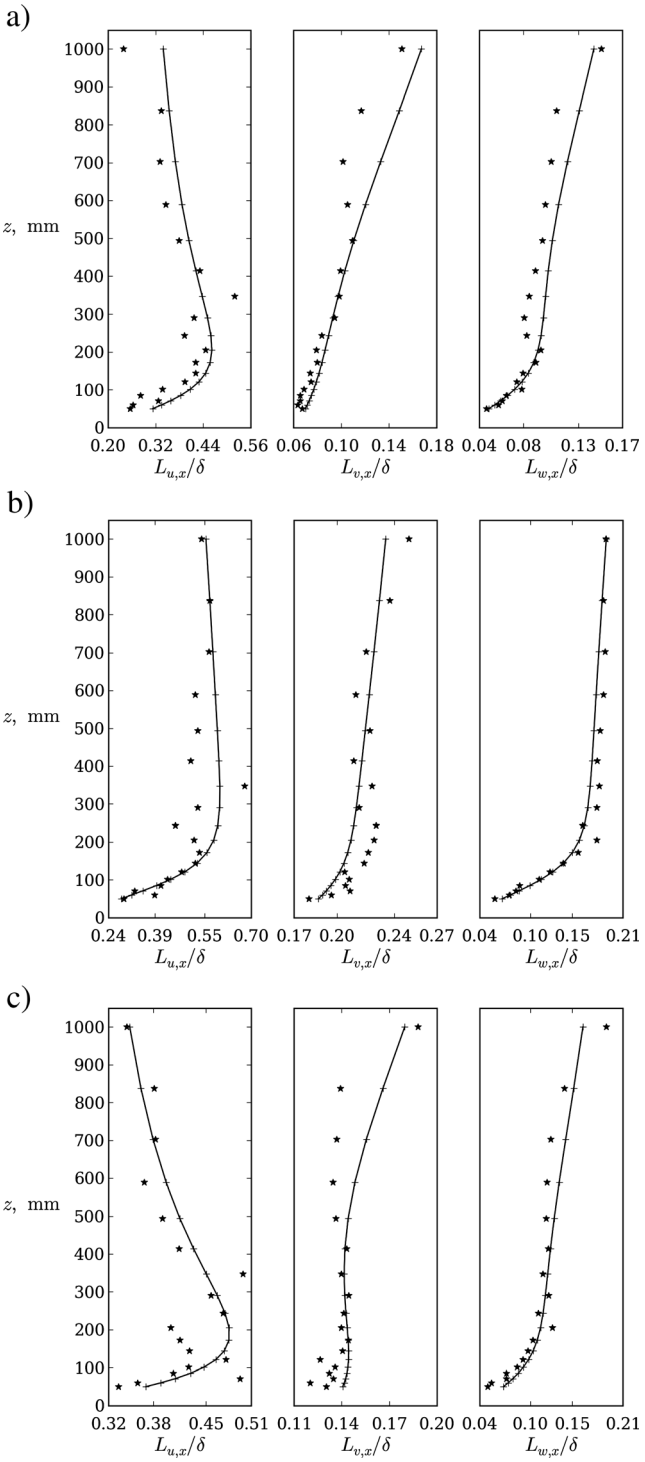

Fig. 6 Comparison of measured turbulence length scales with values estimated by an artificial neural network for **a** urban, **b** suburban, and **c** rural terrain type; *black stars* are experimental results, and *plus signs* on a solid curve are estimated results

While R^2 values obtained for the mean velocity, Reynolds stress, turbulence intensity, and $L_{v,x}$ and $L_{w,x}$ length scales are close to 1, thus indicating good agreement between experiments and ANN estimations, the estimated $L_{u,x}$ turbulence length scales with obtained R^2 is 0.74, which indicates only a moderate but still acceptable agreement between the experiments and estimations. This is due to abrupt changes and data scattering in the profiles of experimental $L_{u,x}$ results; it relates to a common problem to incorporate large eddies into the

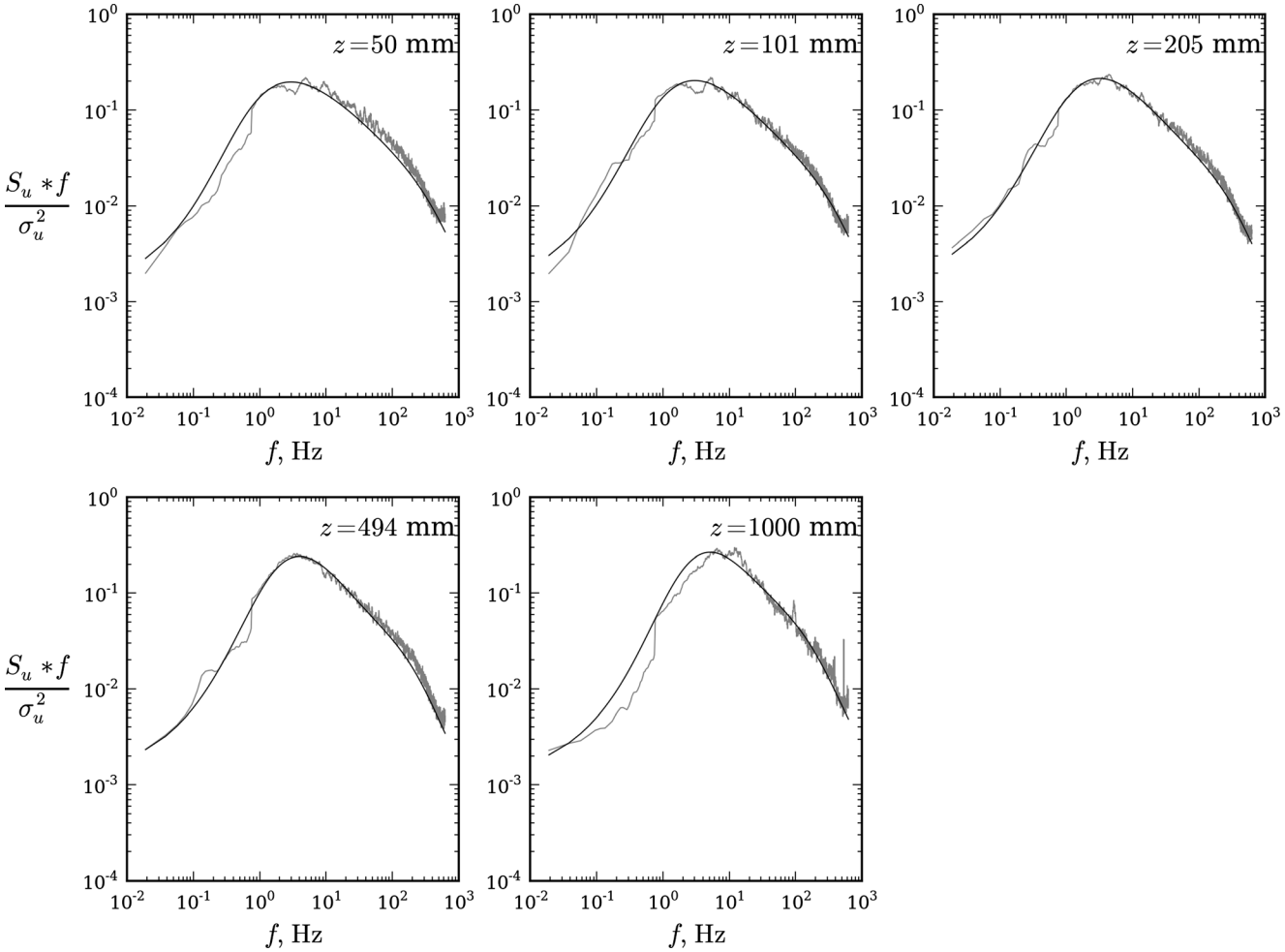

Fig. 7 Comparison of measured power spectral density of longitudinal velocity fluctuations S_u (*gray thin solid curve*) with values estimated by an artificial neural network (*black solid curve*) at 50, 101, 205, 494, and 1,000 mm wind-tunnel scale for urban type of terrain

ABL simulation due to confined cross-section dimensions of the wind-tunnel test section that prevent large eddies to fully develop, e.g., Peterka et al. (1998).

The second ANN estimates S_u, S_v, and S_w power spectral density of velocity fluctuations in the *x*-, *y*-, and *z*-directions, respectively, in 18 different heights and sampled at 5,707 frequencies ranged from 0 to 625 Hz. The input parameters are BBH, SRESD, SREH, frequency (*f*), and *h*. Due to an exponential nature of frequency and power spectral densities, a logarithmic transformation on these variables was performed before importing the data to the ANN. This ANN used configurations 22 and 23 as test dataset (205,388 samples) and the rest of data (configurations 18, 19, 20, and 21) were randomly split to the training and validation dataset in ratio 80:20. This led to the 328,851 samples used for training dataset and 82,053 samples used for validation dataset. After the procedure described in Section 3, the chosen ANN has 2 hidden layers with 12 neurons each. Schematic view of this network is displayed in Fig. 2b and its performance is displayed in Table 3. In Table 3, *RMSE*, *MAE*, and R^2 are nondimensionalized, as well as S_u, S_v, and S_w that were normalized using the respective frequency and variance.

The second ANN estimates the experimental results for the velocity power spectra in all three directions (*x*, *y*, and *z*) with high accuracy, as the observed R^2 values range between 0.94 and 0.97.

4.1 Mean wind velocity

Mean wind velocity profile is an important basic feature in wind engineering, environmental aerodynamics studies, meteorology, etc. It gives information on wind shear with height that is relevant for wind loading of wind turbines, tall buildings, and other complex engineering structures, as well as for dispersion and dilution of air pollutants, air-sea interaction, etc. In the wind-tunnel test section, a velocity profile depends on height and spacing density of surface roughness elements, as well as on vortex generators and barrier wall design. Figure 3 shows a comparison of measured and estimated vertical mean velocity $\overline{u}_z$ profiles normalized with the mean reference velocity $\overline{u}_\delta$ in height δ equal to the BL thickness for three different terrain types.

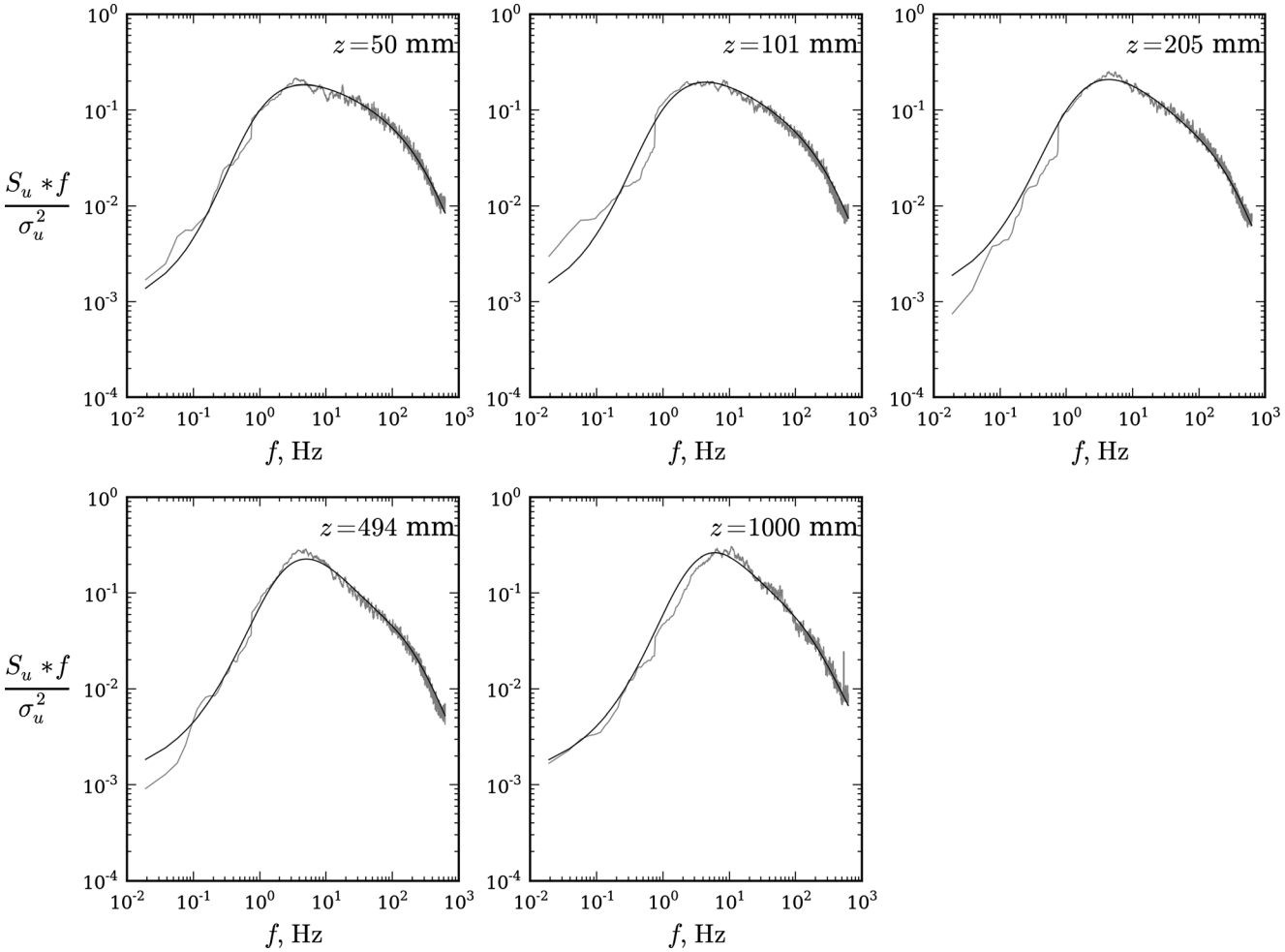

Fig. 8 Comparison of measured power spectral density of longitudinal velocity fluctuations S_u (*gray thin solid curve*) with values estimated by an artificial neural network (*black solid curve*) at 50, 101, 205, 494, and 1,000 mm wind-tunnel scale for rural type of terrain

For urban type terrain, estimated values show very good agreement with the experimental results for the entire BL profile. In the experimental data for suburban and rural type terrain, there is a knick in the profile at about 200-mm height; this creates difficulties for an ANN to make accurate estimations. Therefore, as this sudden change in the measured mean velocity profile is more pronounced, the error in ANN estimation is larger. Nevertheless, an overall estimation made by the ANN for mean velocity profiles can be considered as satisfactory, particularly for engineering purposes, as the wind-tunnel results used here for validation purposes (e.g., Kozmar 2011c) previously proved to be in good agreement with empirical approximation commonly accepted for the ABL flow, i.e., logarithmic law through the surface layer (e.g., Holmes 2007) and the power-law for the entire ABL velocity profile (e.g., Dyrbye and Hansen 1997). In addition, the estimated results agree well with trends obtained by the ANN reported in Varshney and Poddar (2012) and Abdi et al. (2009).

4.2 Turbulence intensity

Turbulence intensity is a particularly important parameter when considering dynamic loading of engineering structures, while it generally needs to be taken into account when studying practically all wind engineering problems. Turbulence intensity in longitudinal and lateral direction can significantly influence vibrations of tall buildings, while bridges are particularly sensitive to vertical turbulence intensity. The I_u, I_v, and I_w turbulence intensity profiles estimated by an ANN are presented in Fig. 4 for urban, suburban, and rural terrain types in comparison with the experimental results.

In general, the estimations made by the ANN are more accurate for built-up environments, as well as for longitudinal turbulence intensity rather than lateral and vertical turbulence intensity. However, all estimated profiles reported in Fig. 4 agree well with the experimental results. Moreover, as the used experimental results (e.g., Kozmar 2011c) previously showed good agreement with the atmospheric conditions (ESDU 74031 1974), it can be adopted

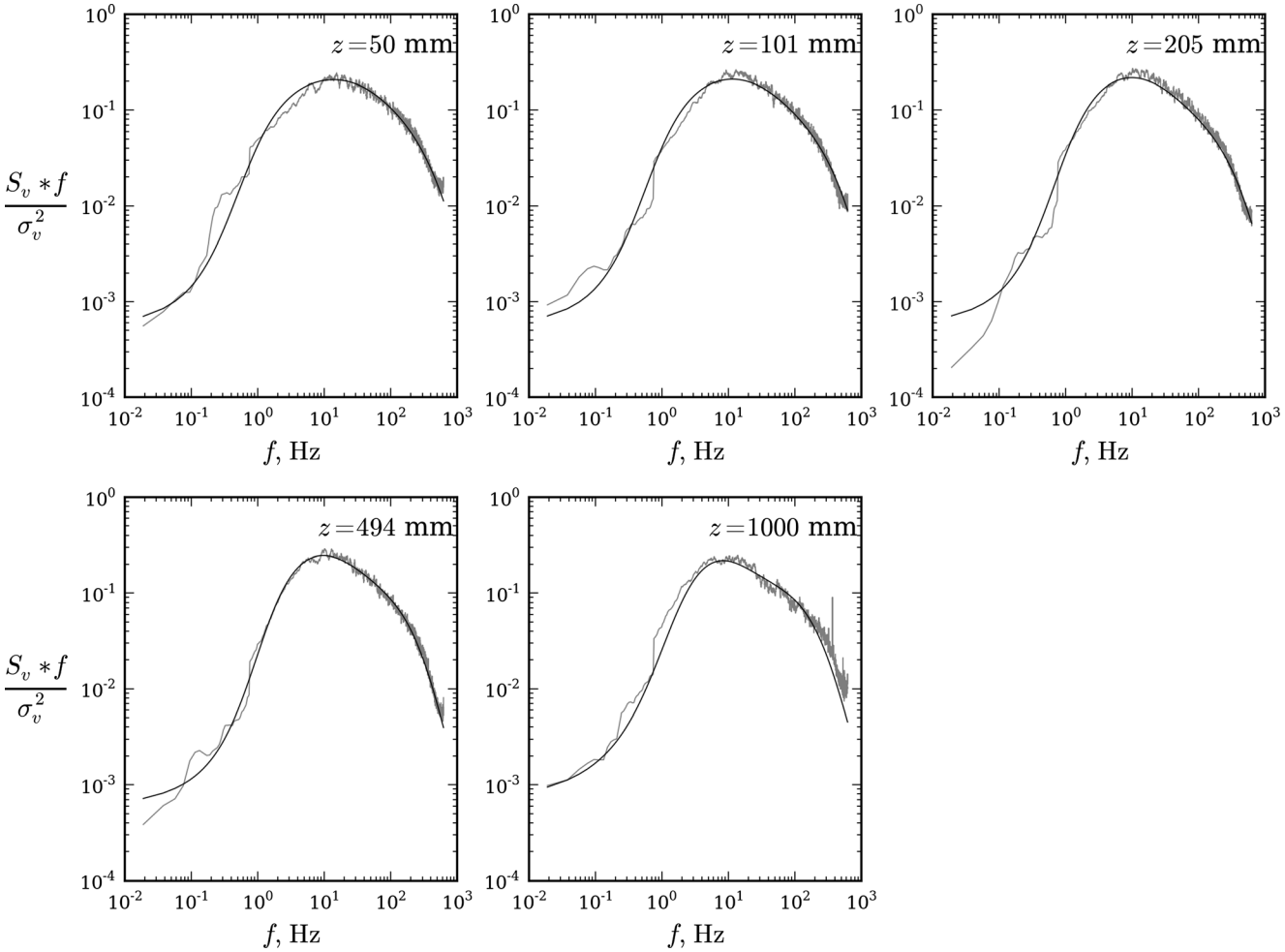

Fig. 9 Comparison of measured power spectral density of lateral velocity fluctuations S_v (*gray thin solid curve*) with values estimated by an artificial neural network (*black solid curve*) at 50, 101, 205, 494, and 1,000 mm wind-tunnel scale for urban type of terrain

that the ANN developed in this study estimates atmospheric turbulence intensity with satisfactory accuracy. Previously, Varshney and Poddar (2012) and Abdi et al. (2009) obtained a good agreement of their ANN estimates with experiments for turbulence intensity in longitudinal direction. However, while they investigated flow and longitudinal turbulence developing above one terrain type only, the ANN developed here make good estimates for turbulence intensity in all three directions (longitudinal, lateral, and vertical) and different terrain types.

4.3 Turbulent Reynolds stress

Turbulent Reynolds stress is one of the major physical mechanisms for vertical heat and mass transfer within the ABL. Hence, its accurate estimation is particularly important in studies dealing with air pollutant dispersion and dilution in urban environments, as previous epidemiologic studies indicated correlations between ambient concentrations of air pollution and adverse health effects, such as respiratory and heart diseases, premature mortality, premature delivery, and low birth weight, e.g., Mohorović (2004), Alebić-Juretić et al. (2007), Kampa and Castanas (2008), Anderson (2009), and Monks et al. (2009). While the Reynolds stress estimation by using the ANN was not under scope in previous relevant studies, the Reynolds stress profiles estimated by an ANN developed here are presented in Fig. 5 for urban, suburban, and rural terrain in comparison with the experimental results.

Similarly to the mean wind velocity profiles, where the knick in measured profiles causes difficulties for an ANN to make accurate estimations, an increased scatter in the experimental Reynolds stress results increases an error margin for ANN when estimating the measured results. Therefore, the estimations made for the urban case are significantly better than for the suburban and rural configurations due to a smaller scatter of the experimental results in this terrain scenario. In particular, the urban wind-tunnel results follow a simple form with a small scatter in comparison with two other cases.

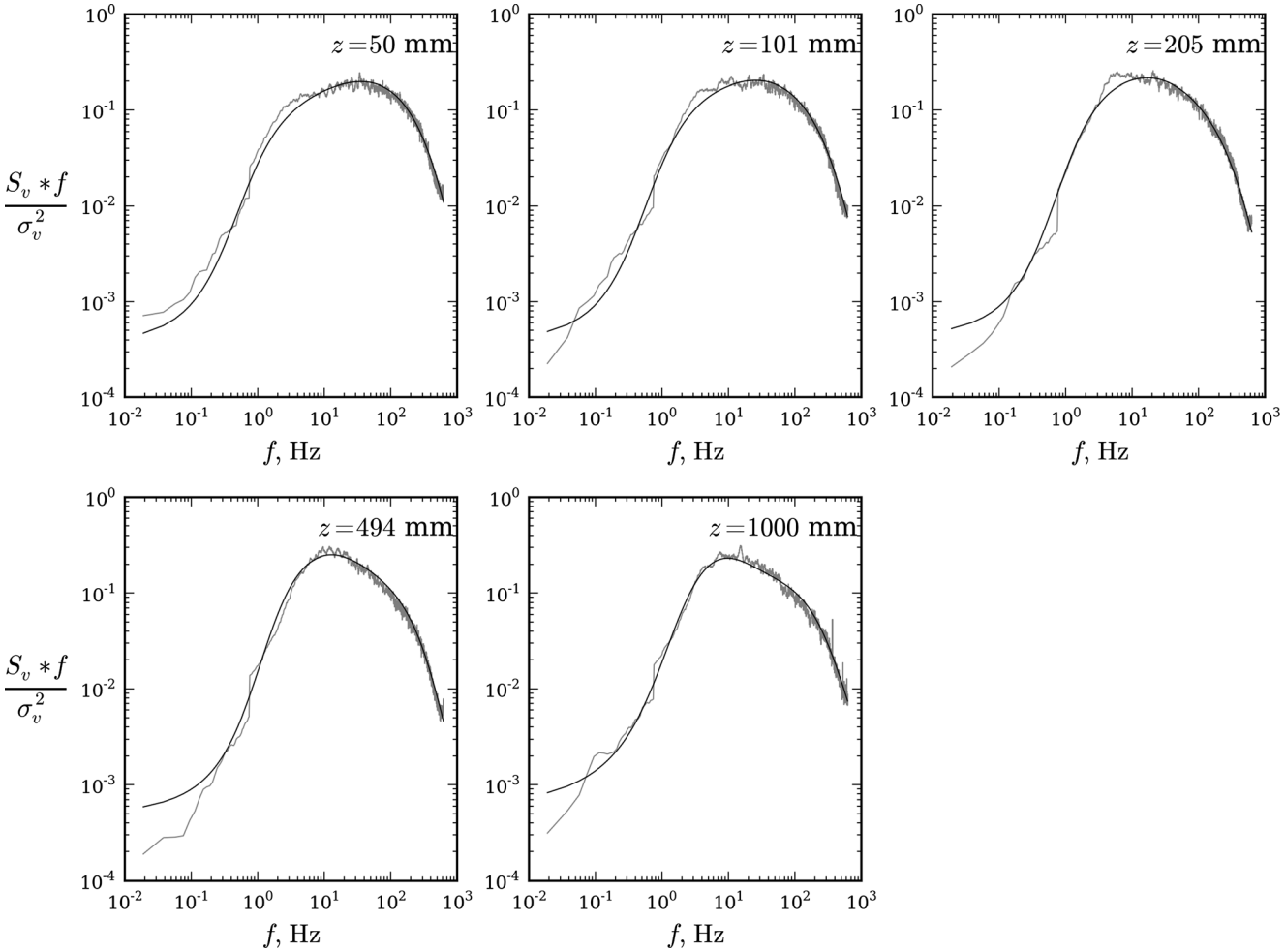

Fig. 10 Comparison of measured power spectral density of lateral velocity fluctuations S_v (*gray thin solid curve*) with values estimated by an artificial neural network (*black solid curve*) at 50, 101, 205, 494, and 1,000 mm wind-tunnel scale for rural type of terrain

4.4 Turbulence length scales

Turbulence length scales represent an average size of turbulent eddies within the ABL flow. It is particularly important to know their characteristics when designing engineering structures, as eddies of different sizes wrap around the structures in a different way; therefore, they can create different structural loads. As up to the authors' best knowledge, in this "wind tunnel–ANN way," the turbulence length scales have not been tackled yet, this leads directly to the one of the main contributions of this study. The turbulence length scales estimated by an ANN are presented in Fig. 6 for urban, suburban, and rural terrain types in comparison with the experimental results.

In general, the estimated results are in good agreement with the experiments. However, as the $L_{u,x}$ experimental results are scattered more than that for $L_{v,x}$ and $L_{w,x}$ turbulence length scales, the estimations for $L_{u,x}$ profiles are not as good as those for $L_{v,x}$ and $L_{w,x}$ profiles. This is in agreement with performance of ANN observed in this study for other turbulence parameters as well. In addition, it needs to be mentioned that it is generally difficult to fully recreate turbulence length scales in the wind tunnel, as observed in full-scale, which is due to essentially confined boundaries of the wind-tunnel test section that do not allow large eddies to develop more fully.

4.5 Power spectral density of velocity fluctuations

While the knowledge of integral turbulence parameters is more or less sufficient for many aerodynamic problems, in dealing with complex fluid–structure interactions, it is of high importance to gain insight into the distribution of turbulent kinetic energy across a wide range of frequencies as well. For that purpose, the power spectral density of velocity fluctuations commonly serves as a widely adopted parameter describing features of atmospheric turbulence. Longitudinal and lateral power spectra are commonly considered important for tall and slender structures, while vertical power spectra are important when considering aerodynamic performance of bridges. In this study, all three power spectra are considered

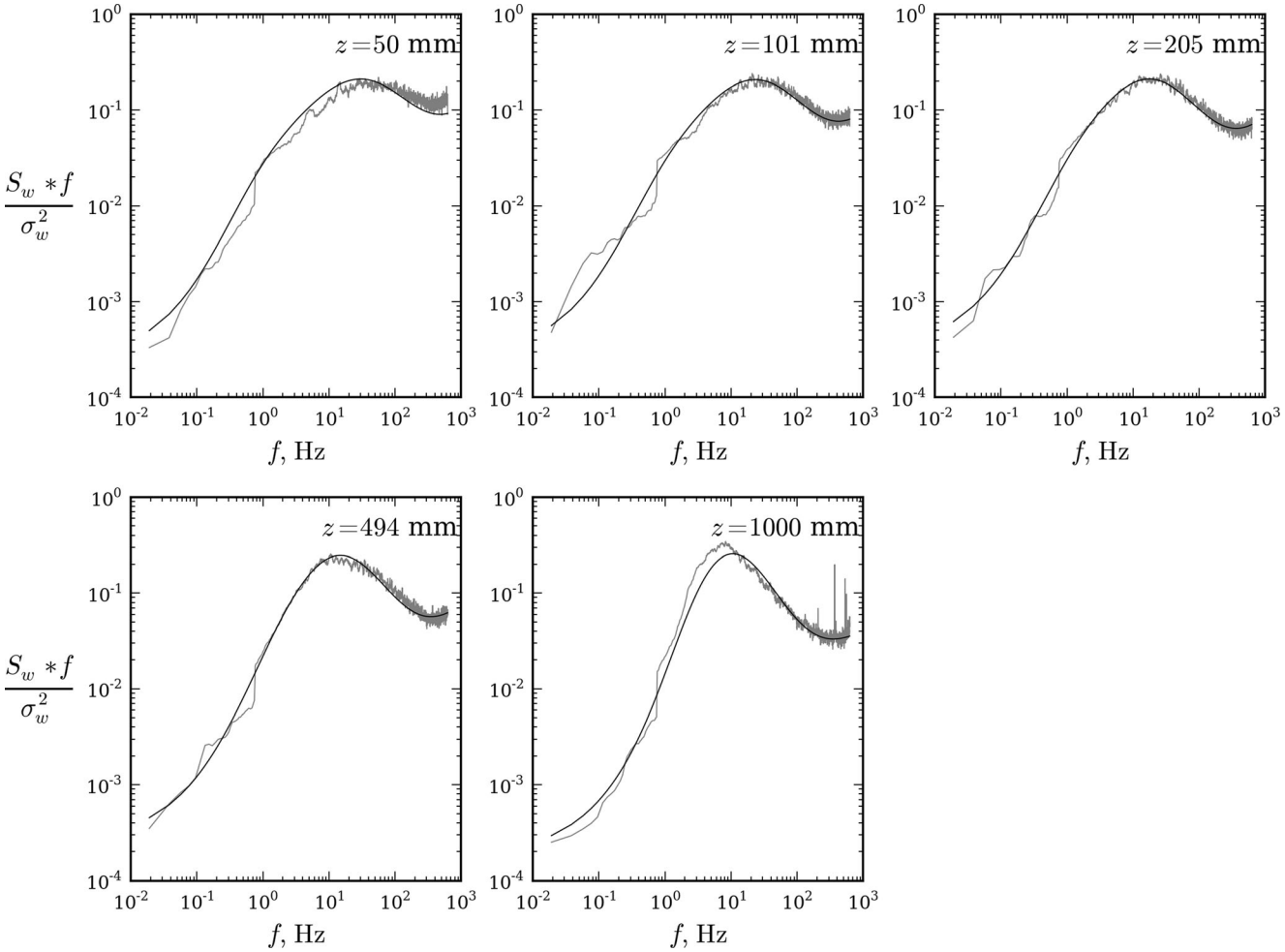

Fig. 11 Comparison of measured power spectral density of vertical velocity fluctuations S_w (*gray thin solid curve*) with values estimated by an artificial neural network (*black solid curve*) at 50, 101, 205, 494, and 1,000 mm wind-tunnel scale for urban type of terrain

and reported for five selected heights distributed throughout the ABL simulation, i.e., at 50, 101, 205, 494, and 1,000 mm wind-tunnel scale. The S_u, S_v, and S_w power spectra estimated by an ANN are presented in Figs. 7, 8, 9, 10, 11, and 12 for urban and rural terrain in comparison with the experimental results, while the wind-tunnel results for suburban terrain exposure are not available.

In all the tests performed, the estimated curves agree well with the experimental results, particularly in the high-frequency range (Kolmogorov inertial subrange), due to more sampling points available in high- than in low-frequency range that allows for a better training of the second ANN. In addition, the created ANN estimations can be adopted to be in good agreement with the atmospheric turbulence, as the wind-tunnel velocity power spectra in *x*-,*y*-, and *z*-directions used here for validation purposes previously proved to be in good agreement with commonly adopted design curve by von Kármán (1948) and the inertial subrange energy dissipation law by Kolmogorov (1941). While previously, Varshney and Poddar (2012) obtained a good estimate of their ANN with the longitudinal velocity power spectra only; in this study, this was achieved in all three directions, i.e., longitudinal, lateral, and vertical.

5 Concluding remarks

Two different artificial neural networks (ANNs) are developed in order to enable quick and time-efficient designing of experimental hardware for the atmospheric boundary layer (ABL) simulations in the wind tunnel. A standard ANN procedure is used in order to further investigate best-practice possibilities with this approach rather than to attempt to improve ANN designing methodology. The scope was to estimate an optimal design of the Counihan hardware, i.e., castellated barrier wall, vortex generators, and surface roughness, in order to simulate the ABL flow developing above urban, suburban, and rural terrain types, as previous studies were performed for one terrain type only. Basic barrier height,

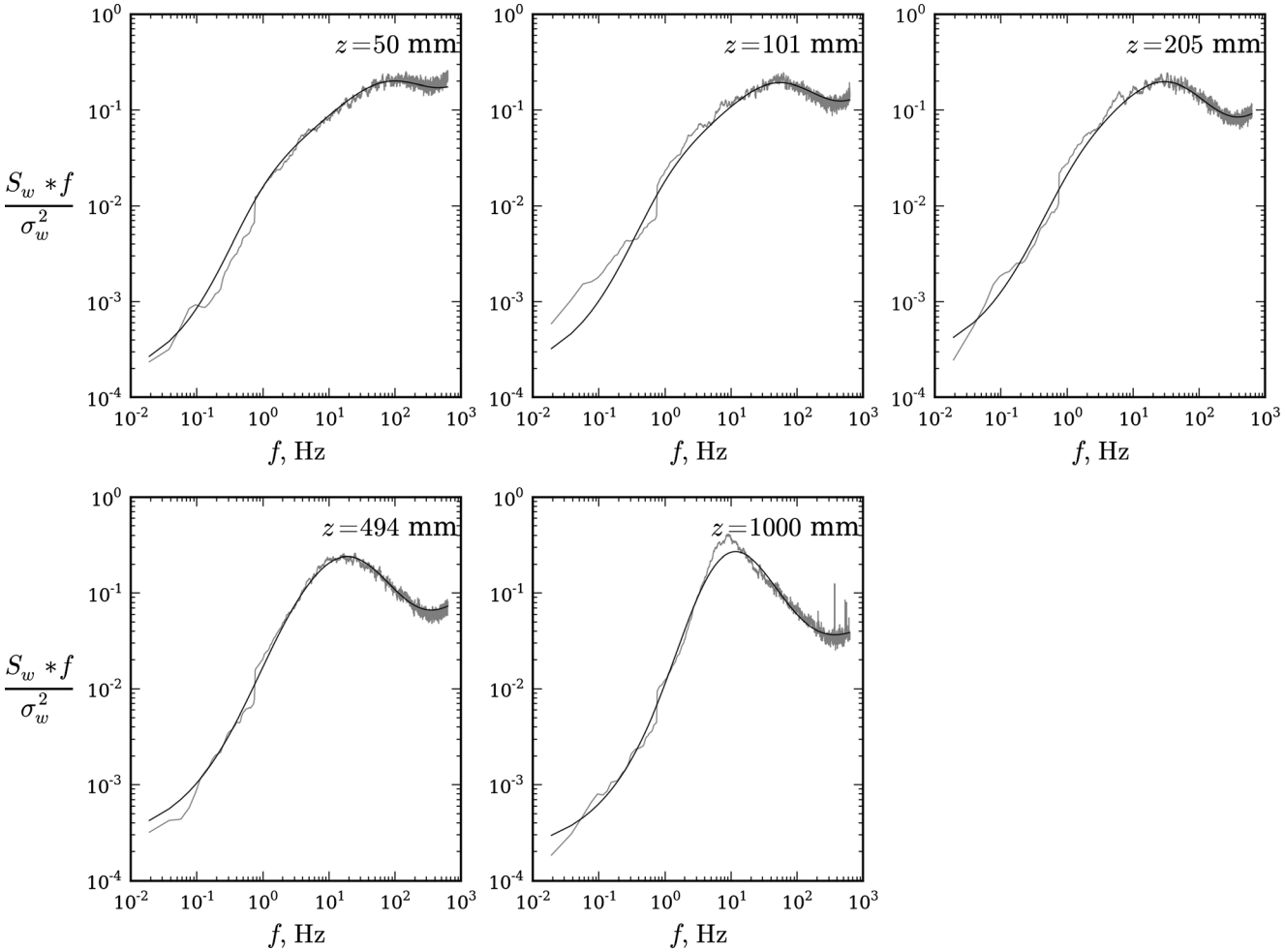

Fig. 12 Comparison of measured power spectral density of vertical velocity fluctuations S_w (*gray thin solid curve*) with values estimated by an artificial neural network (*black solid curve*) at 50, 101, 205, 494, and 1,000 mm wind-tunnel scale for rural type of terrain

barrier castellation height, spacing density, and height of surface roughness elements are the parameters that were varied to create satisfactory ABL simulations. This modeling approach was designed to allow for estimating parameters that describe wind flow and atmospheric turbulence, i.e., mean wind velocity, turbulent Reynolds stress, turbulence intensity, turbulence length scales, and power spectral density of velocity fluctuations. This extensive set of studied flow and turbulence parameters is unmatched in comparison to the previous relevant studies, as it includes turbulence intensity and power spectral density of velocity fluctuations in all three directions, as well as the Reynolds stress profiles and turbulence length scales. Modeling results created using ANNs are validated with an extensive set of ABL wind-tunnel simulations.

In general, the modeling results agree well with the experiments for all three terrain types, particularly in the lower ABL within the height range of the most of engineering structures, as well as for urban type terrain types. Moreover, ANNs indicate sensitivity to abrupt changes and data scattering in profiles of wind-tunnel results. The proposed and largely novel approach allows for quicker achieving targeted flow and turbulence features of the ABL wind-tunnel simulations than that is the case with the common trial and error procedure. This approach is expected to enable wind-tunnel modelers a time-efficient design of ABL simulations in studies dealing with air pollutant dispersion, wind loading of structures, wind energy, and urban micrometeorology and microclimatology. Future work will need to address ANN modeling with reversed input and output parameters, as to further investigate this approach for engineering applications.

Acknowledgments JK and GG acknowledge Mrs. Sanja Grgurić for her assistance and support, as well as the Gekom Ltd. Company. HK acknowledges support of the Croatian Ministry of Science and Technology, the German Academic Exchange Service (DAAD), and the Croatian Academy of Sciences and Arts (HAZU) for wind-tunnel testing at the Institute of Aerodynamics and Fluid Mechanics, Faculty of Mechanical Engineering, Technische Universität München; the helpful discussions with Prof. Boris Laschka, Dr. Albert Pernpeintner, and Dr. Joseph Fischer; and the TUM technical staff for the manufacturing of the simulation hardware, and in part the University of Zagreb grant 05206–2. BG acknowledges the Croatian Ministry and the Croatian National Science Foundation for support through projects BORA, 119-1193086-1311 and CATURBO, 09/151, respectively.

References

Abdi D, Levine S, Bitsuamlak G (2009) Application of an artificial neural network model for boundary layer wind tunnel profile development. Proc 11th American Conf Wind Eng, San Juan, Puerto Rico

Alebić-Juretić A, Cvitaš T, Kezele N, Klasinc L, Pehnec G, Šorgo G (2007) Atmospheric particulate matter and ozone under heat-wave conditions: do they cause an increase of mortality in Croatia? Bull Environ Contam Toxicol 79:468–471

Anderson HR (2009) Air pollution and mortality: a history. Atmos Environ 43:142–152

Antonić O, Križan J, Marki A, Bukovec D (2001) Spatio-temporal interpolation of climatic variables over large region of complex terrain using neural networks. Ecol Model 138:255–263

Baklanov A, Grisogono B, Bornstein R, Mahrt L, Zilitinkevich S, Taylor P, Larsen S, Rotach M, Fernando HJS (2011) The nature, theory and modeling of atmospheric planetary boundary layers. Bull Am Meteorol Soc 92:123–128

Balendra T, Shah DA, Tey KL, Kong SK (2002) Evaluation of flow characteristics in the NUS-HDB wind tunnel. J Wind Eng Ind Aerodyn 90(6):675–688

Bishop C (1995) Neural Networks for Pattern Recognition. Oxford University Press, Oxford

Bitsuamlak G, Stathopoulos T, Bédard C (2006) Effects of upstream two-dimensional hills on design wind loads: a computational approach. Wind Struct 9(1):37–58

Bitsuamlak GT, Bédard C, Stathopoulos T (2007) Modeling the effect of topography on wind flow using a combined numerical–neural network approach. ASCE J Comput Civ Eng 21:384–392

Bottou LY (1998) Reconnaissance de la Parole par Reseaux Multi-Couches. Proceedings of the International Workshop on Neural Networks and Their Applications (NeuroNimes), 197–217

Brunskill AW, Lubitz WD (2012) A neural network shelter model for small wind turbine siting near single obstacles. Wind Struct 15(1):43–64

Chen Y, Kopp GA, Surry D (2003) Prediction of pressure coefficients on roofs of low buildings using artificial neural networks. J Wind Eng Ind Aerodyn 91:423–444

Cook NJ (1978) Determination of the model scale factor in wind-tunnel simulations of the adiabatic atmospheric boundary layer. J Wind Eng Ind Aerodyn 2:311–321

Counihan J (1969) An improved method of simulating an atmospheric boundary layer in a wind tunnel. Atmos Environ 3(2):197–214

Dyrbye C, Hansen SO (1997) Wind loads on structures. John Wiley & Sons, New York

English E, Fricke F (1999) The interference index and its prediction using a neural network analysis of wind-tunnel data. J Wind Eng Ind Aerodyn 83:567–575

Esau I (2010) On application of artificial neural network methods in large-eddy simulations with unresolved urban surfaces. Mod Appl Sci 4:3–11

ESDU 74031 (1974) Characteristics of atmospheric turbulence near the ground, Part II: single point data for strong winds (neutral atmosphere). Engineering Sciences Data Unit 74031

Fu JY, Li Q, Xie Z (2006) Prediction of wind loads on a large flat roof using fuzzy neural networks. Eng Struct 28:153–161

Fu JY, Liang SG, Li QS (2007) Prediction of wind-induced pressures on a large gymnasium roof using artificial neural networks. Comput Struct 85:179–192

Holmes JD (2007) Wind loading of structures. Taylor & Francis, UK

Huang P, Gu M (2005) Experimental study on wind-induced dynamic interference effects between two tall buildings. Wind Struct 8(3):147–161

Hucho WH (2002) Aerodynamik der stumpfen Körper. Vieweg & Sohn, Wiesbaden

Irwin HPAH (1981) The design of spires for wind simulation. J Wind Eng Ind Aerodyn 7:361–366

Kampa M, Castanas E (2008) Human health effects of air pollution. Environ Pollut 151:362–367

Khanduri AC, Bédard C, Stathopoulos T (1997) Modelling wind-induced interference effects using back propagation neural networks. J Wind Eng Ind Aerodyn 72:71–79

Kolmogorov AN (1941) The local structure of turbulence in incompressible viscous fluid for very large Reynolds numbers. Proc Acad Sci USSR 30:299–303

Kozmar H (2008) Influence of spacing between buildings on wind characteristics above rural and suburban areas. Wind Struct 11(5):413–426

Kozmar H (2010) Scale effects in wind tunnel modeling of an urban atmospheric boundary layer. Theor Appl Climatol 100(1–2):153–162

Kozmar H (2011a) Wind-tunnel simulations of the suburban ABL and comparison with international standards. Wind Struct 14:15–34

Kozmar H (2011b) Truncated vortex generators for part-depth wind-tunnel simulations of the atmospheric boundary layer flow. J Wind Eng Ind Aerodyn 99:130–136

Kozmar H (2011c) Characteristics of natural wind simulations in the TUM boundary layer wind tunnel. Theor Appl Climatol 106:95–104

Kozmar H (2012a) Physical modeling of complex airflows developing above rural terrains. Environ Fluid Mech 12:209–225

Kozmar H (2012b) Improved experimental simulation of wind characteristics around tall buildings. J Aerosp Eng 25:670–679

Kwatra N, Godbole PN, Krishna P (2002) Application of artificial neural network for determination of wind induced pressures on gable roof. Wind Struct 5(1):1–14

Mohorović L (2004) First two months of pregnancy—critical time for preterm delivery and low birthweight caused by adverse effects of coal combustion toxics. Early Hum Dev 80:115–123

Monks PS, Granier C, Fuzzi S, Stohl A, Williams ML et al (2009) Atmospheric composition change—global and regional air quality. Atmos Environ 43:5268–5350

Peterka JA, Hosoya N, Dodge S, Cochran L, Cermak JE (1998) Area average peak pressures in a gable roof vortex region. J Wind Eng Ind Aerodyn 77–78(1):205–215

Plate EJ (1982) Engineering Meteorology. Elsevier Scientific Publishing Company, Amsterdam, New York

Riedmiller M, Braun H (1993) A direct adaptive method for faster backpropagation learning: The RPROP Algorithm. Proc IEEE Int Conf Neural Networks

Schlichting H, Gersten K (1997) Grenzschicht-Theorie. Springer, Berlin

Sockel H (1984) Aerodynamik der Bauwerke. Vieweg & Sohn, Braunschweig

Sousa S, Martins F, Alvim-Ferraz M, Pereira M (2007) Multiple linear regression and artificial neural networks based on principal components to predict ozone concentrations. Environ Model Softw 22:97–103

Varshney K, Poddar K (2012) Prediction of wind properties in urban environments using artificial neural network. Theor Appl Climatol 107:579–590

Von Kármán T (1948) Progress in the statistical theory of turbulence. Proc Natl Acad Sci USA 34(11):530–539

Vujić B, Vukmirović S, Vujić G, Jović N, Jović G, Babić M (2010) Experimental and artificial neural network approach for forecasting of traffic air pollution in urban areas: the case of Subotica. Therm Sci 14:221–230

Wojciechowski M (2011) Feed-forward neural network for python. Dept Civ Eng Arch Env Eng, Technical University of Lodz, Poland, http://ffnet.sourceforge.net/

Xie ZN, Gu M (2005) A correlation-based analysis on wind-induced interference effects between two tall buildings. Wind Struct 8(3):163–178

Yasushi U, Tsuruishi R (2008) Wind load evaluation system for the design of roof cladding of spherical domes. J Wind Eng Ind Aerodyn 96:2054–2066